Abstract: The present work focuses on the development of novel
injectable, self-gelling composite hydrogels based on two types of low
esterified amidated pectins from citrus peels and apple pomace. Sol-gel-
derived, calcium-rich bioactive glass (BG) fillers in a particle form are
applied as delivery vehicles for the release of Ca2+ ions to induce
internal gelation of pectins.
Composites were prepared by a relatively simple mixing technique, using
20% w/v BG particles of two different sizes (2.5 and <45 μm). Smaller
particles accelerated pectin gelation slightly faster than bigger ones,
which appears to result from the higher rate of Ca2+ ion release. μCT
showed inhomogeneous distribution of the BG particles within the
hydrogels. All composite hydrogels exhibited strong antibacterial
activity against methicilin-resistant Staphylococcus aureus. The
mineralization process of pectin-BG composite hydrogels occurred upon
incubation in simulated body fluid for 28 days. In vitro studies
demonstrated cytocompatibility of composite hydrogels with MC3T3-E1
osteoblastic cells.

Cover Letter

18th October 2018

Dear Professor M.A. Coimbra,

Thank you for giving us the chance to submit a revision.

We are pleased to submit revised manuscript entitled *Pectin-bioactive glass self-gelling, injectable composites with high antibacterial activity*.

The manuscript has been improved according to the Reviewers' suggestions. Red font indicates where changes have been made. We really hope that this manuscript will be acceptable for publication in ***Carbohydrate Polymers***.

Many thanks for your attention and we look forward to hearing from you.

Yours sincerely

Michal Dziadek (corresponding author) and Co-authors

Pectin-BG composite hydrogels were prepared by a relatively simple mixing technique

BG particles delivers Ca^{2+} ions for internal pectin crosslinking

Composite hydrogels exhibited strong antibacterial activity against MRSA

Mineralization process of composite hydrogels occurred upon incubation in SBF

Composite hydrogels were cytocompatible with MC3T3-E1 osteoblastic cells

We were grateful to receive all the valuable comments from the Reviewers. The manuscript has been improved according to the Reviewers' suggestions. Red font indicates where changes have been made. We really hope that this manuscript will be acceptable for publication in *Carbohydrate Polymers*.

Below you will find our detailed answers to the Reviewers' comments and suggestions.

Reviewer 1

Fig. 1 A1 and A2 :Axis need modification(vertical...)

Figures 1 A1 and A2 have been modified according to the Reviewer's suggestion.

Reviewer 2

I am afraid that the manuscript is not suitable for publication in its current state since some major issues I raised last time are still not resolved properly (e.g. comments 1,3 and 6), which greatly affect the scientific quality of the manuscript.

1. In abstract and conclusion, the authors claim that BG release Ca2+ ions to crosslink pectin, are there any evidences? If no, it is not proper to make this statement.

   We have conducted extra experiments to demonstrate Ca^{2+} release from BG. ICP-OES analysis of ddH$_2$O after 5-minute incubation of BG particles (the ratio of BG particles to ddH$_2$O was the same as that of BG particles to pectin solution during the preparation process of hydrogels – 200 mg/1 ml) proved massive release of Ca^{2+} ions. The results of ICP-OES analysis and some comments have been added to the Discussion, Conclusion and Abstract sections.

3. Page 10, lines 20-23: "The results of representative rheometric measurements of pectin-BG hydrogel composites are shown in Figure 1B. The storage modulus (G`) reached a plateau value after 5 minutes, indicating that gelation process did not depend on pectin type (AA, CA) and BG particle size (2.5 <mu>m, <45 <mu>m). All of the composite hydrogels exhibited similar storage modulus values, suggesting comparable stiffness." The descriptions are not consistent with the data in Figure 1B. The discussion is thus not proper, so as that on Page 19, line 9.

The results and discussion of rheometric measurements have been revised and improved according to the Reviewer's suggestion. Some comment has also been included in the Conclusion and the Abstract sections.

6. Page 13, lines 1-3: "the great majority of the cells seeded on the composite hydrogels and in their vicinity remained viable, indicating low cytotoxicity. Significantly larger numbers of the cells were observed in vicinity of the composite hydrogels than on them." So (1) please indicate where the hydrogels are in Figure 3A; (2) since more cells are growing on the plate rather than on hydrogels, what the results of Figure 3B really mean? Please discuss.

The MTS results presented on Figure 3B represent metabolic activity of the cells seeded on materials and also on TCPS in their vicinity. The results of microscopic observations and metabolic activity of the cells indicate that although the MC3T3-E1 cells did not adhere to the surface of hydrogels to a great extent, they exhibited good viability and proliferation in the presence of materials. Such tests are often used in biomaterials testing because they allows one to check how cells behave not only on the biomaterial surface but also in its vicinity − we can observe whether a material releases toxic products or generates toxic debris, both of which can affect metabolic activity of the cells.

We have added appropriate text to the Results section.

Dear Reviewer 2,

Thank you for your suggestions for improvement. We hope that you are now satisfied with our responses. If not, we would be grateful if you would provide some more details concerning your comments and suggestions. This would help us to improve the manuscript and ensure high scientific quality. Many thanks in advance.

Yours sincerely

Michal Dziadek

1   *Pectin-bioactive glass self-gelling, injectable composites with high*

2   *antibacterial activity*

3

4   Timothy E.L. Douglas[1,2,3], Michal Dziadek[2,4]*, Josefien Schietse[1], Matthieu Boone[5], Heidi A.

5   Declercq[6], Tom Coenye[7], Valérie Vanhoorne[8], Chris Vervaet[8], Lieve Balcaen[9], Maria

6   Buchweitz[10], Frank Vanhaecke[9], Frederic Van Assche[5], Katarzyna Cholewa-Kowalska[4],

7   Andre G. Skirtach[1]

8

9   [1]Dept. Biotechology, Ghent University, Belgium, [2]Engineering Dept., Lancaster University,

10   United Kingdom, [3]Materials Science Institute (MSI), Lancaster University, United Kingdom,

11   [4]Dept. Glass Technology and Amorphous Coatings, AGH University of Science and

12   Technology, Krakow, Poland, [5]Dept. Physics and Astronomy, Ghent University, Belgium,

13   [6]Tissue Engineering group, Ghent University, Belgium, [7]Laboratory of Pharmaceutical

14   Microbiology, Ghent University, Belgium, [8]Laboratory of Pharmaceutical Technology, Ghent

15   University, Belgium, [9]Dept. Chemistry, Ghent University, Belgium, [10]Institute of

16   Biomaterials, Dept. Analytical Food Science, University of Stuttgart, Germany

17   *Corresponding Author. Email: dziadek@agh.edu.pl

18

19

1   **Abstract**

2   The present work focuses on the development of novel injectable, self-gelling composite

3   hydrogels based on two types of low esterified amidated pectins from citrus peels and apple

4   pomace. Sol-gel-derived, calcium-rich bioactive glass (BG) fillers in a particle form are

5   applied as delivery vehicles for the release of Ca^{2+} ions to induce internal gelation of pectins.

6   Composites were prepared by a relatively simple mixing technique, using 20% w/v BG

7   particles of two different sizes (2.5 and <45 μm). Smaller particles accelerated pectin gelation

8   slightly faster than bigger ones, which appears to result from the higher rate of Ca^{2+} ion

9   release. μCT showed inhomogeneous distribution of the BG particles within the hydrogels.

10   All composite hydrogels exhibited strong antibacterial activity against methicilin-resistant

11   *Staphylococcus aureus*. The mineralization process of pectin-BG composite hydrogels

12   occurred upon incubation in simulated body fluid for 28 days. *In vitro* studies demonstrated

13   cytocompatibility of composite hydrogels with MC3T3-E1 osteoblastic cells.

14

15   **Keywords:** hydrogel; pectin; bioactive glass; antibacterial; bone tissue engineering

16

1. Introduction

Hydrogels possess many advantages that make them suitable as 3D scaffolds for tissue engineering applications. They are structurally similar to native extracellular matrix, can serve as delivery vehicles for growth factors and drugs, and may be delivered in a minimally invasive way (Stratton, Shelke, Hoshino, Rudraiah, & Kumbar, 2016). Pectin is one of the natural polymers that is receiving increased attention as a hydrogel material for tissue engineering, as well as drug and cell delivery systems, primarily as a result of its high tissue-like water content, providing an ideal micro-environment for cellular proliferation and differentiation, good biocompatibility, and biodegradability (Fabiola Munarin et al., 2014; Neves et al., 2015). Furthermore, pectins have been reported to exhibit a wide range of biological activities, such as antioxidant, antitumor and anti-inflammatory properties (Cui et al., 2017; Popov et al., 2016). These natural hydrogels hold great promise, mostly because of the implantation by minimally invasive surgery as injectable, self-gelling systems (F. Munarin et al., 2011; Popov et al., 2016).

Pectins are derived mainly from by-products of juice and cider industry, therefore, they represent a group of environmentally friendly raw materials that can be used for production of hydrogel biomaterials (Neves et al., 2015). Pectins are water soluble, anionic polysaccharides composed of α-(1-4) ᴅ-galacturonic acid units (GalA) extracted from plant cell walls. They are widely used in food industry as thickeners or gelling agents. Currently apple pomace and citrus peels are the two main sources of commercial pectins. Based on their degree of esterification (DE), pectins are classified as high methoxyl pectin (HM, DE > 50%) or low-methoxyl pectin (LM, DE < 50%). LM is capable to form a hydrogel in the presence of divalent ions, such as calcium ions, over a wider range of pH values. In fact, the methoxyl groups can be converted to amide groups, which modify some properties of the pectin gels. Amidated LM pectins require less calcium for hydrogel formation, and they are also less

1   prone to precipitation at high Ca^{2+} concentrations (Secchi et al., 2014; Yuliarti, Hoon, &

2   Chong, 2017b, 2017a).

3   Functionalization of hydrogels and polymer coatings with particles brings additional

4   functionalities (Volodkin, Delcea, Möhwald, & Skirtach, 2009), including crosslinking, which

5   was shown to affect the elasticity, Young's modulus, and the cell adhesion (Francius et al.,

6   2006). In regard with hydrogels, one of the approaches to induce crosslinking of anionic

7   polysaccharide, including pectins, is the so-called internal gelation, employing such inorganic

8   fillers as $CaCO_3$ and hydroxyapatite in particle form. These inorganic fillers are dispersed in

9   polymer solution and act as delivery vehicles for slow release of Ca^{2+} ions, which crosslink

10   the polymer solution leading to the formation of a homogeneous hydrogel network (Moreira

11   et al., 2014; F. Munarin et al., 2015; Fabiola Munarin et al., 2014; Neves et al., 2015; Secchi

12   et al., 2014).

13   Another inorganic particles, proposed in this study, that can be used as a source of Ca^{2+} ions

14   for internal gelation are bioactive glasses. Bioactive glass particles also possess several

15   suitable characteristics. Moreover, bioactive glasses are able to bond to living bone through

16   the formation of a surface layer of hydroxyapatite (HAp) in contact with the body fluids, as a

17   result of their high reactivity in aqueous media. It was also shown that ionic dissolution

18   products (Si and Ca) of bioactive glasses can lead to favorable intracellular and extracellular

19   responses, actively stimulating bone formation (Bosetti, Zanardi, Hench, & Cannas, 2003;

20   Hench, 2009; Silver, Deas, & Erecińska, 2001). Other advantages of bioactive glasses include

21   their antibacterial properties against a wide range of pathogenic bacteria (Munukka et al.,

22   2008; Nazemi, Mehdikhani-Nahrkhalaji, Haghbin-Nazarpak, Staji, & Kalani, 2016; Zhang et

23   al., 2010).

24   Therefore, bioactive glass fillers can impart antibacterial and osteogenic properties to the

25   hydrogels, and also induce their mineralization with HAp upon incubation in biologically

relevant fluids or *in situ* after implantation. Furthermore, combining the inorganic fillers with the hydrogel polymer matrix can be used as a strategy to improve mechanical properties of the injectable biomaterials. All of these make pectin-BG composite hydrogels good candidates for bone tissue engineering applications.

The aim of this work is focused on the development of novel injectable, self-gelling composite hydrogels, using an internal gelation method and employing two types of low esterified amidated pectins from citrus peels and apple pomace as an organic matrix. The novelty of this work is to apply sol-gel-derived, calcium-rich bioactive glass particles of two sizes, namely 2.5 μm and <45 μm, as an inorganic filler to induce internal pectin crosslinking. As mentioned above, citrus and apple are the two most common sources of pectin. The following properties were evaluated: gelation ability and kinetics (i); distribution of BG particles within the composite hydrogels (ii); composite hydrogel antibacterial activity against methicilin-resistant *Staphylococcus aureus* (MRSA) (iii); *in vitro* MC3T3-E1 osteoblastic cell response (iv), and composite hydrogel mineralization process upon incubation in simulated body fluid (v). It was hypothesized that the different particle sizes of the inorganic filler, i.e. the bioactive glass particles, would affect the properties described above.

2. Materials and Methods

2.1 Materials

Two types of low esterified amidated (AM) pectins (Herbstreith & Fox, Neuenbürg, Germany) from citrus peels (CA; degree of esterification = 27.4%, degree of amidation = 22.8%, galacturonic acid content = 93.5%) and apple pomace (AA; degree of esterification = 27.9% , degree of amidation = 22.3.%, galacturonic acid content = 86.7%) were used.

All materials were obtained from Sigma-Aldrich, unless stated otherwise.

5

2.2 Bioactive glass particle synthesis and characterization

2.2.1 Bioactive glass synthesis

Bioactive glass (BG) of the following composition (mol%): $40SiO_2-54CaO-6P_2O_5$, was produced using the sol–gel method as described previously (Laczka, Cholewa, & Laczka-Osyczka, 1997). Tetraethoxysilane (TEOS; $Si(OC_2H_5)_4$), triethylphosphate (TEP; $OP(OC_2H_5)_3$), and calcium nitrate tetra-hydrate ($Ca(NO_3)_2·4H_2O$) (POCh, Poland) were used as basic components of the sol–gel process. 1M HCl solution (POCh, Poland) was used as a catalyst in the hydrolysis and condensation reactions and ethanol (96%; POCh, Poland) was used as a solvent. The formed gel was gradually dried at temperature, increasing in the range from 40 to 120°C for 7 days and then subjected to thermal treatment at 700°C for 20 h. Two glass particle sizes were obtained: <45 μm by grinding and sieving and 2.5 μm by milling in an attritor with ZrO_2 balls in isopropyl alcohol medium.

2.2.2 Microparticle size distribution measurements

Microparticle size distributions were measured by laser diffraction (Mastersizer-S long bench, Malvern Instruments, Malvern, UK), using the wet dispersion technique. The powder (about 100 mg) was dispersed in 10 ml of a 0.1% w/v aqueous polysorbate 80 solution. The resulting suspension was added to the MS1 Small Volume Dispersion unit (Malvern Instruments, Malvern, UK) in order to obtain an obscuration of the laser beam of approximately 20%. The microparticle size distribution was measured using the following parameters: 300RF lens, 2.4 mm active beam length, 1500 rpm stirrer speed, 6000 scans, polydisperse analysis model.

2.3 Production of hydrogel-bioactive glass composites and rheometry

Briefly, 1 ml pre-autoclaved (121°C for 15 minutes) aqueous 0.8% w/v AA or CA pectin solution was mixed with 200 mg pre-autoclaved bioactive glass particles of 2.5 μm or <45 μm

1 sizes at room temperature and shaken vigorously to obtain 20% w/v pectin-BG composite

2 hydrogels, denoted as AA-2.5, AA-45, CA-2.5, CA-45, respectively.

3 Gelation rate was investigated using an AR1000N Rheometer (TA Instruments, USA). All

4 experiments were performed at 37º C, at strain 1% and frequency 1 Hz using a plate-cone

5 setup with a stainless steel plate and an acrylic cone of 4 cm diameter.

6 The release of Ca^{2+} from BG particles was monitored by ICP-OES measurements (Plasm 40,

7 Perkin Elmer, USA), conducted after incubation of BG particles in ddH_2O for 5 minutes. The

8 ratio of BG particles to ddH_2O was the same as BG particles to pectin solution during the

9 preparation process of the composite hydrogels (200 mg/1 mL).

10

11 **2.4 High-resolution X-ray tomography**

12 The distribution of particles inside pectin–BG composite hydrogels was examined using high-

13 resolution X-ray tomography (μCT). The datasets were acquired at the HECTOR scanner

14 (Masschaele et al., 2013) of the Ghent University Centre for X-ray Tomography (UGCT;

15 www.ugct.ugent.be). The XWT 240-SE (X-RAY WorX, Germany) X-ray tube was operated

16 at $90\,kV_p$ at a target power of 10 W which results in a focal spot size below 4 μm. For

17 detection a PerkinElmer 1620 CN3 CS flat panel detector was used at an exposure time of 1s

18 per projection. For each measurement, 1200 projection images were taken over a 360° angular

19 range. The source sample distance and source detector distance were set to 3.21 cm and 96.71

20 cm, respectively, resulting a magnification of approximately 30 and thus a voxel size of

21 6.54×6.54 μm². The total field-of-view was approximately 9×10 mm². The acquired

22 radiographs were reconstructed using the software package Octopus (XRE, Gent, Belgium)

23 and visualized using VGStudioMax (Volume Graphics GmbH, Heidelberg, Germany).

24

25

1 *2.5 Antibacterial testing*

2 To evaluate antibacterial properties, composite hydrogels of volume 1 ml were submerged

3 with a silicone disc in 1 ml containing 10^4 CFU (colony-forming unit) methicilin-resistant

4 *Staphylococcus aureus* (MRSA) Mu50 in Mueller-Hinton broth. The disc served as a

5 substrate for MRSA attachment and growth. After 24 h incubation at 37°C, composite

6 hydrogels and medium were removed, and discs were washed with physiological saline to

7 remove non-adhered bacteria. Discs were collected and the number of CFU per silicone discs

8 was determined by plating. Silicone discs without added composite hydrogels served as

9 a control. For all sample groups, n = 3.

10

11 *2.6 Cell biological characterization with osteoblastic cells*

12 *2.6.1 Cell culture on composites*

13 Composite hydrogels were cast under sterile conditions in wells of 12-well cell culture plates,

14 1 ml per well. 6-mm discs were cut out using a sterile hole punch and were used for cell

15 culture experiments. The prepared sterile materials were placed at the bottom of 48-well

16 culture plate wells. MC3T3-E1 Subclone 4 cells (ATCC, USA) were seeded on the composite

17 hydrogels at a density of $2 \cdot 10^4$ cells/well and cultured for 24 h in 1 ml complete culture

18 medium (MEM α supplemented with 10% FBS, Gibco, USA) at 37°C in a humidified, 5%

19 CO_2 atmosphere. Afterwards, MTT assay (Vybrant® MTT Cell Proliferation Assay Kit,

20 Thermo Fisher Scientific, USA) and live/dead staining (Calcein AM/propidium iodide,

21 Thermo Fisher Scientific, USA) were performed according to the manufacturer's protocols.

22 For all sample groups, n = 3.

23

24 *2.6.2 Testing of eluates from composite hydrogels*

1   To produce eluates, the sterile composite hydrogels were incubated in complete culture

2   medium at 37 °C for 24 h. The ratio of the composite hydrogel's weight (g) and solution's

3   volume (ml) was 20/100. MC3T3-E1 Subclone 4 cells were seeded on the bottom of 96-well

4   plate at a density of $1.5 \cdot 10^{4}$ cells/well and cultured for 24 h in eluates (undiluted, $5\times$ and $10\times$

5   diluted with complete culture medium) at 37°C in a humidified, 5% CO_2 atmosphere.

6   Afterwards, MTT assay (Vybrant[®] MTT Cell Proliferation Assay Kit, Thermo Fisher

7   Scientific, USA) was performed according to the manufacturer's protocol. For all sample

8   groups, n = 3.

9

10   *2.7. Mineralization studies in SBF*

11   *2.7.1. SBF preparation and sample incubation*

12   The mineralization process of pectin-bioactive glass composites was performed by incubation

13   in simulated body fluid (SBF) prepared according to Kokubo (Kokubo et al., 1990). The

14   composite hydrogels were immersed in SBF solution and incubated at 37 °C in separate

15   containers for 28 days under sterile conditions. The ratio of the composite hydrogel's weight

16   (g) and solution's volume (ml) was 1/100. Afterwards the composite hydrogels were taken out

17   of SBF, frozen at -24 °C and subsequently subjected to a lyophylization process in order to

18   obtain dry mass. Freeze-drying was performed using FreeZone 6 Liter Freeze Dry System

19   (Labconco, USA) for 48 hours.

20

21   *2.7.2. Monitoring of the mineralization process: FTIR, SEM/EDX, ICP-OES*

22   Before and after mineralization experiments and subsequent lyophilization, the structure of

23   the composite hydrogels was examined using FTIR. Spectra were recorded with a Vertex 70v

24   spectrometer (Bruker, USA) using KBr technique. Spectra were collected in the range 4000–

25   400 cm^{-1} and 128 scans were accumulated at 4 cm^{-1} resolution.

Morphology and elemental analysis of all freeze-dried composite hydrogels before and after mineralization in SBF were determined using SEM (Nova NanoSEM 200 FEI Europe Company, accelerating voltage 15 kV) coupled with an energy dispersion X-ray (EDX) analyzer. Materials were analyzed after coating with a thin conductive carbon layer.

Elemental composition of composite hydrogels was determined using ICP-OES as described previously (Douglas et al., 2012). An ICP-OES technique (Plasm 40, Perkin Elmer, USA) was also used to investigate the changes in ion concentration in the SBF after 28 days of composite hydrogel incubation. Media were analyzed before and after material incubation (Dziadek, Zagrajczuk, Menaszek, & Cholewa-Kowalska, 2018). For all sample groups, n = 3.

2.8. Statistical analysis

The results were analyzed using one-way analysis of variance (ANOVA) with Duncan post hoc tests, which were performed with Statistica 13.1 (Dell Inc., USA) software. The results were considered statistically significant when $p<0.05$.

3. Results

3.1 Bioactive glass particle characterization and formation of pectin-bioactive glass composite hydrogels

The results of laser diffraction analysis of BG particles are shown in Table 1 and Figure 1A. Smaller BG particles (denoted as 2.5 µm) revealed D[v ; 0.5] values of 2.24 µm, while larger-sized BG particles (denoted as <45 µm) showed D[v ; 0.9] values of 42.62 µm. D[v ; 0.1], D[v ; 0.5] and D[v ; 0.9] defines the diameter (based on the volume distribution of the particles) at which 10%, 50% and 90% of the particles are smaller than this diameter.

The results of representative rheometric measurements of pectin-BG hydrogel composites are shown in Figure 1B. In the case of composite hydrogels containing BG particles of 2.5 μm size, the storage modulus (G`) reached a plateau value within 1 minute, while for CA-45 and AA-45 a plateau was observed after approximately 5 and 10 minutes, respectively. All of the composite hydrogels exhibited similar storage modulus values, suggesting comparable stiffness.
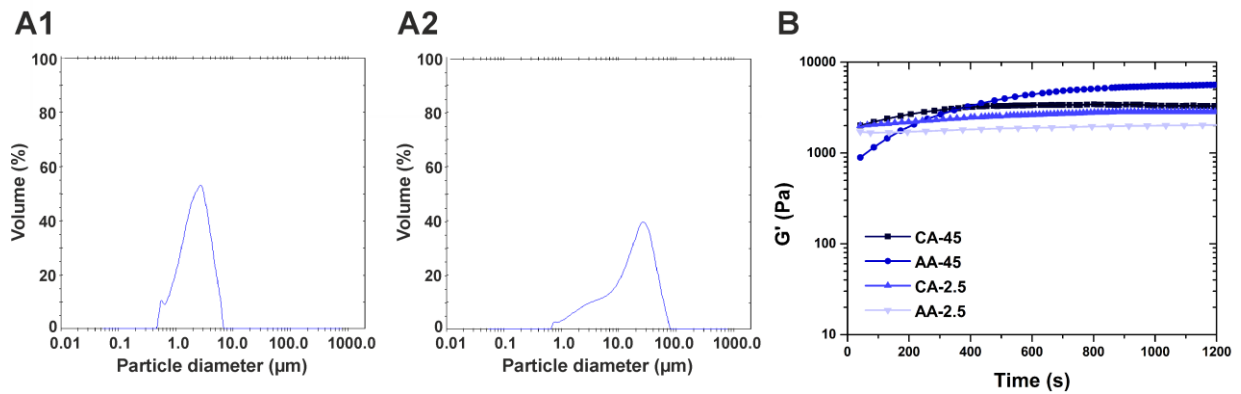
Figure 1. Size distributions of bioactive glass particles denoted as 2.5 μm (A1) and <45 μm (A2) measured by laser diffraction. Gelation kinetics of pectin-BG composite hydrogels measured by rheometry (B).

Table 1. Laser diffraction analysis of bioactive glass particles.

BG	D[v ; 0.1]	D[v ; 0.5]	D[v ; 0.9]
2.5 μm	0.95 μm	2.24 μm	4.32 μm
<45 μm	2.77 μm	18.18 μm	42.62 μm

1 *3.2 μCT examination*

2 Images of transverse and longitudinal sections of pectin-BG composite hydrogels are shown

3 in Figure 2. It can be seen that BG aggregates of different sizes were present, and that these

4 aggregates were not uniformly distributed throughout the CA and AA pectin composite

5 hydrogels. It seems that bigger BG particles (<45 μm) are distributed more homogeneously

6 than smaller ones (2.5 μm), which is especially noticeable in the case of the AA-45 composite

7 hydrogel.

8
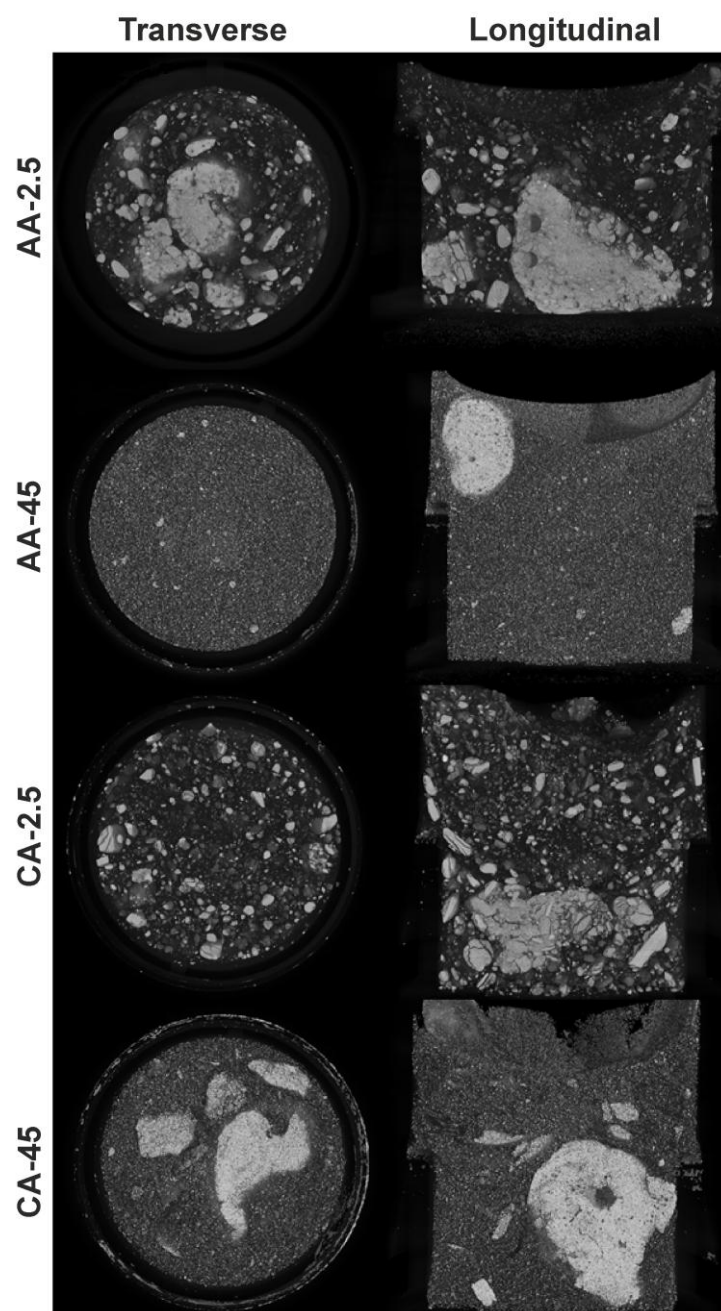
Figure 2. µCT-based visualization of pectin-BG composite hydrogels: transverse and longitudinal sections. The diameter material of the transverse slices is 8.2 mm; on the longitudinal slices this corresponds with the lower part of the sample.

3.3 In vitro osteoblastic cell response

Fluorescence images of live/dead staining of MC3T3-E1 osteoblastic cells cultured for 24 h in direct contact with pectin-BG composite hydrogels are presented in Figure 3A. The results showed that the great majority of the cells seeded on the composite hydrogels and in their vicinity remained viable, indicating low cytotoxicity. Significantly larger numbers of the cells were observed in vicinity of the composite hydrogels than on them. MC3T3-E1 osteoblastic cells were well spread with proper morphology and numerous cytoplasmic extensions, characteristic for osteoblastic cells, indicating good cell adhesion and viability.
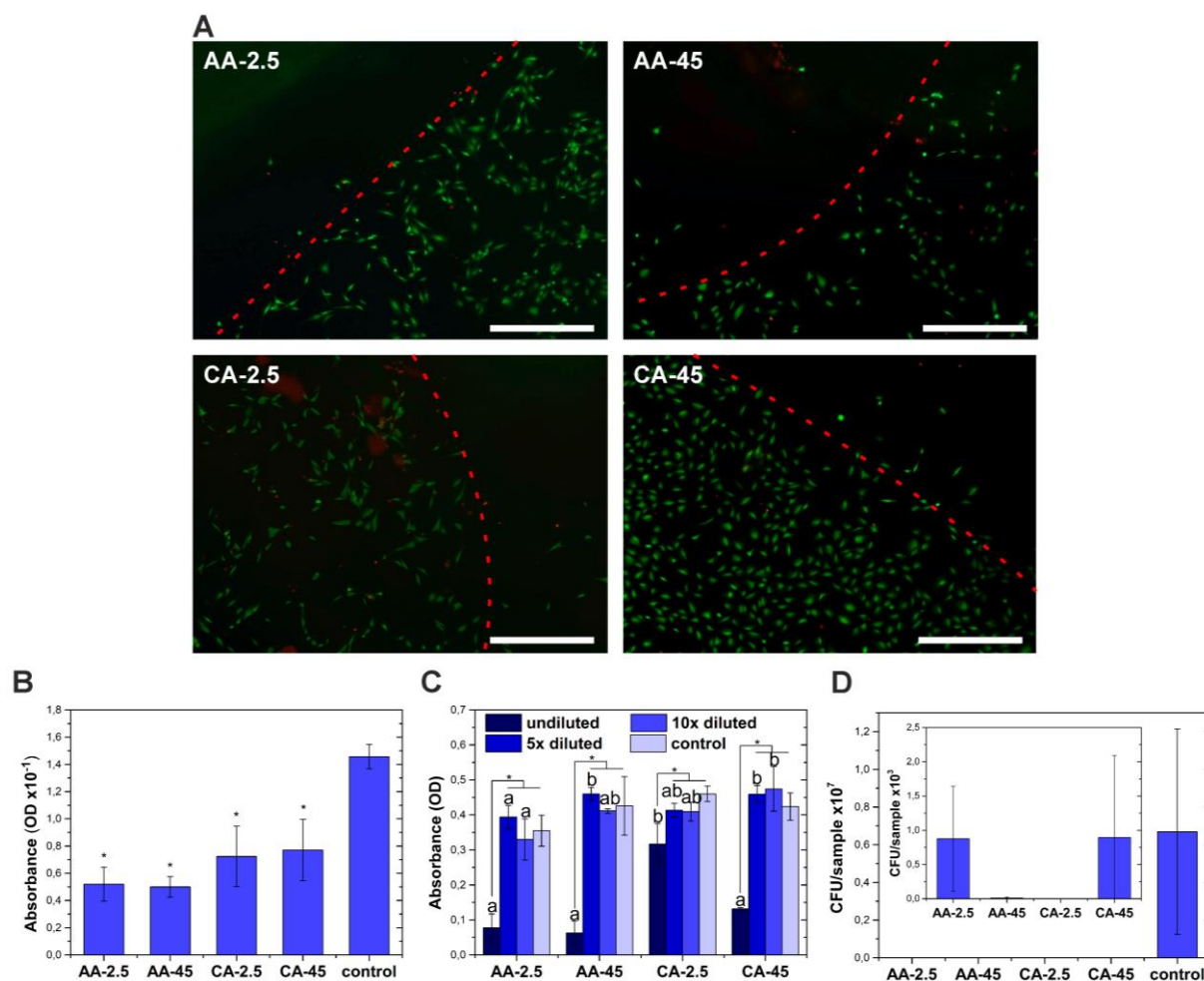
Figure 3. Fluorescence images of live/dead staining of MC3T3-E1 cells cultured for 24 h in direct contact with composite hydrogels (A). Scale bar = 500 µm in all images. Red dash lines indicate where the hydrogels are. Metabolic activity (assessed by MTT assay) of the cells cultured for 24 h directly on composite hydrogels (B). Statistically significant differences (p <0.05) relative to the control are indicated by *. Metabolic activity (assessed by MTT assay) of the cells cultured for 24 h in eluates from composite hydrogels, undiluted and diluted by factors of 5 and 10 (C). Statistically significant differences (p <0.05) between dilutions of specific material eluent and control are indicated by *, between different material eluents in specific dilution are indicated by a-b. Colony-forming unit (CFU) of MRSA strain Mu50 cultured in the presence of composite hydrogels (D). All results are expressed as mean ±SD.

14

Metabolic activity of the MC3T3-E1 osteoblastic cells cultured for 24 h in direct contact with composite hydrogels, corresponding to their number, is shown in Figure 3B. These results represent metabolic activity of the cells seeded on composite hydrogels and also on TCPS in their vicinity. The values recorded for all of the pectin-BG composites were significantly lower compared to the control (TCPS). Metabolic activity of the osteoblastic cells cultured in direct contact with composite hydrogels consisting of CA tended to be higher compared to those in contact with AA-2.5 and AA-45, however, the difference was not statistically significant. These results correspond with fluorescence images of live/dead staining of the cells (Figure 3A).

The results of microscopic observations and metabolic activity of the cells indicate that although the MC3T3-E1 cells did not adhere to the surface of composite hydrogels to a great extent, they exhibited good viability and proliferation in the presence of composite hydrogels. Cell number after culture for 24 h in material eluates is shown in Figure 3C. The results showed that the number of osteoblastic cells in all undiluted eluates was significantly lower compared to cells in 5× and 10× diluted eluates and on controls, for which the values did not differ significantly from each other. However, the cells cultured in undiluted eluate from CA-2.5 hydrogel exhibited significantly higher metabolic activity in comparison with other undiluted eluates. When considering 5× and 10× diluted eluates, the numbers of cells tended to be at a similar level.

*3.4 Antibacterial testing*

The results of antibacterial testing are shown in Figure 3D. The mean values recorded for all pectin-BG composites are four orders of magnitude smaller than value for control, indicating strong antibacterial activity against MRSA. Antibacterial properties did not depend on BG particle size (2.5 µm, <45 µm) or pectin type (AA, CA).

3.5 Mineralization of composite hydrogels in SBF

SEM images and EDX spectra of pectin-BG composite hydrogels before and after 28-day

incubation in SBF are shown in Figure 4. After incubation in SBF, all of the pectin-BG

composite hydrogels showed morphological changes characteristic for precipitation of

calcium phosphate (CaP), namely the appearance of spherical, "cauliflower-like" deposits

with fine morphology rich in calcium (Ca) and phosphorus (P). The detected amount of

silicon (Si), derived from BG particles, was greatly reduced, indicating that the mineralization

was in an advanced stage. Furthermore, EDX analysis indicated small amounts of sodium

(Na) and chlorine (Cl) incorporated into hydrogels from SBF solution.
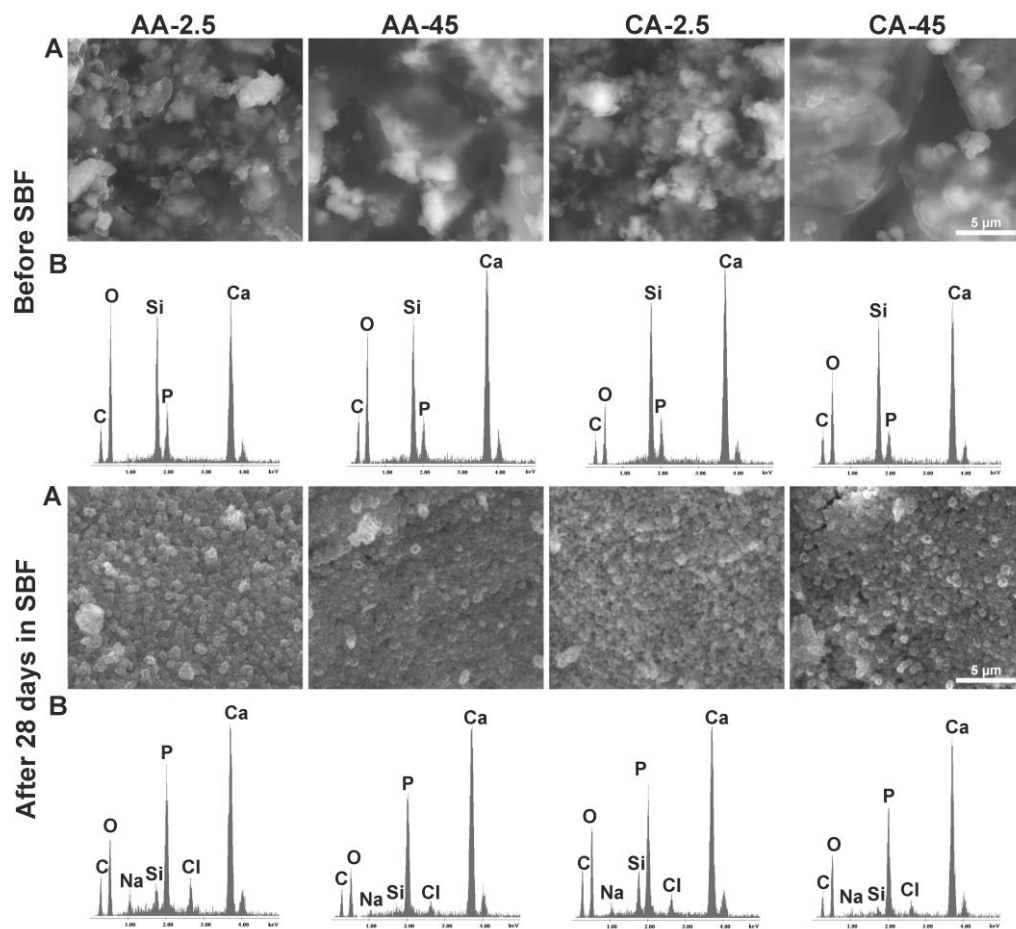
Figure 4. SEM images (A) and EDX spectra averaged for the entire analyzed surface (B) of

pectin-bioactive glass composite hydrogels before and after 28-day incubation in SBF.

1 FTIR spectra of pectin-BG composite hydrogels before and after 28 days of incubation in

2 SBF are shown in Figure 5. Incubation in SBF resulted in visible changes in the IR absorption

3 spectra of the materials. Two bands in the range of 560 – 605 cm^{-1} and band at 470 cm^{-1},

4 corresponding to v^4 in-plane bending and v^4 out-of-plane bending of PO_4^{3-} groups,

5 respectively, became more visible, and the band at approximately 1030 cm^{-1}, corresponding to

6 v^4 antisymmetric stretching of PO_4^{3-} groups, became more intense and narrower (Kim, Kim,

7 Kim, Akaike, & Kim, 2002). Additionally, the shoulder at 1220 cm^{-1} became more intense

8 and new band of low intensity at 800 cm^{-1} appeared, which may be due to silica groups in the

9 CaP/silica gel layer formed during incubation in SBF. The appearance of the aforementioned

10 bands points to the formation of crystalline form of calcium phosphate, most likely calcium-

11 deficient hydroxyapatite (CDHA).
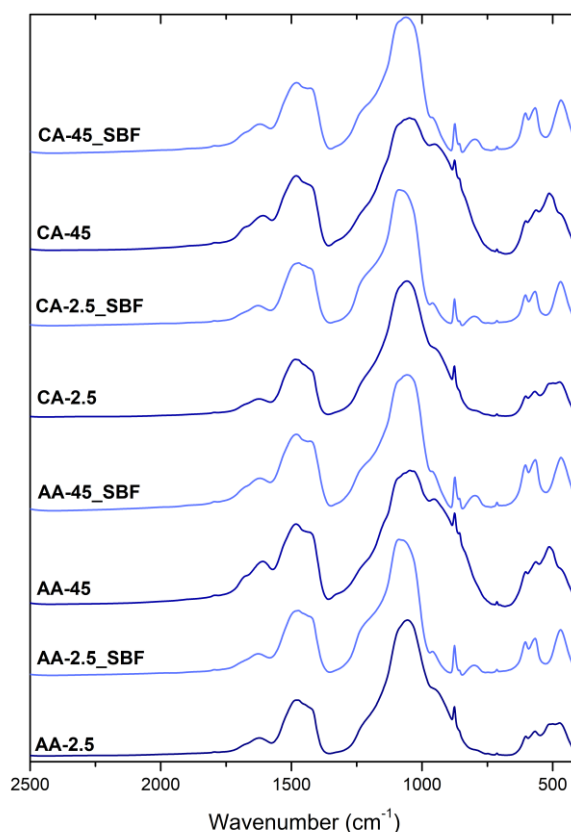
12

13 **Figure 5.** FTIR spectra of pectin-bioactive glass composite hydrogels before and after

14 incubation in SBF for 28 days.

1   Ca, P and Si concentrations in SBF and pH values after incubation of pectin-BG composite

2   hydrogels are presented in Figure 6A. The results showed that Ca concentration in SBF

3   depended on BG particle size (2.5 μm, <45 μm), but was not correlated with pectin type (AA,

4   CA). The increase in Ca content was observed for all of the composite hydrogels. However,

5   composite hydrogels containing BG particles of <45 μm size showed higher changes. These

6   changes correlated with pH values of SBF. An increase in pH was induced by calcium release

7   from glass structure, therefore higher Ca concentrations in SBF resulted in higher increase in

8   pH for AA-45 and CA-45 composite hydrogels. Simultaneously, an almost total reduction in

9   P concentration for materials with BG particles of 2.5 μm size and significant decrease for

10   hydrogels containing BG particles of <45 μm size was observed, confirming the intensive

11   mineralization of all composite hydrogels. The release of Si from the material structure was

12   noticed, however this process surprisingly did not depend on BG particle size or pectin type.
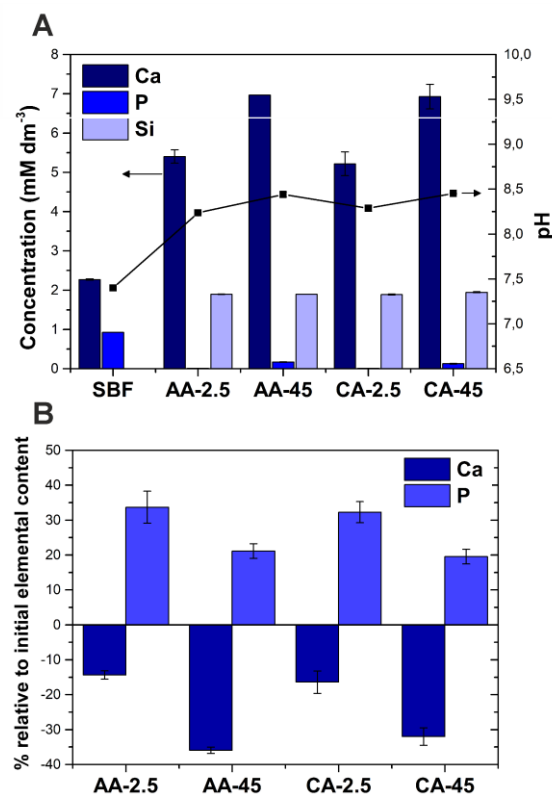
13

14   **Figure 6.** Ca, P and Si concentrations and pH values after incubation of composite hydrogels

15   in SBF for 28 days (standard deviation is invisible for some results) (A). % of elements

present in sample after 28 days incubation in SBF relative to elemental content before incubation (B).

The changes of Ca and P content in samples after 28 days incubation in SBF relative to the theoretical elemental content before incubation are shown in Figure 6B. The decrease in Ca concentration in all of the samples was observed, however a higher reduction was recorded for composite hydrogels containing BG particles of <45 μm size. All of the composite hydrogels showed increases in P content. Nevertheless, composite hydrogels containing BG particles of 2.5 μm size exhibited higher increases in P than hydrogels containing BG particles of <45 μm size. These results correlate closely with Ca and P concentrations in SBF (Figure 6A).

4. Discussion

In the present work the effect of incorporation of sol-gel-derived, calcium-rich bioactive glass particles of two different sizes, namely 2.5 μm and <45 μm, into citrus and apple low esterified amidated pectins was investigated. To date, there is no research examining these kinds of composite systems. The following properties of the resulting composite hydrogels were studied: gelation ability and kinetics (i); distribution of BG particles within the composite hydrogels (ii); composite hydrogel antibacterial activity (iii); *in vitro* osteoblastic cell response (iv), and composite hydrogel mineralization process upon incubation in SBF (v).

4.1 Formation of pectin-bioactive glass composites and μCT examination

The results showed that gel-derived, calcium-rich BG particles are a sufficiently rich source of Ca^{2+} ions for inducing internal gelation of CA and AA amidated pectins through an ionic crosslinking mechanism with acceptable time frame for injection.

In other works, the production of self-gelling injectable pectin hydrogels by internal gelation using calcium carbonate was also proposed (Moreira et al., 2014; Neves et al., 2015; Secchi et al., 2014). In these studies, modification of pH was necessary to enable gelation. This required addition of a further substance to modify pH. One advantage of the system provided in the present study is that no addition of pH modifiers is necessary.

In this work, an influence of BG particle size on gelling kinetics could be observed (Figure 1B) – smaller particles (<2.5 μm) accelerate gelation slightly faster than bigger ones (<45 μm). This is consistent with previous works, in which other inorganic sources of Ca^{2+} ions, namely synthetic hydroxyapatite (HAp) micro- and nanoparticles were used to crosslink low esterified citrus pectin (F. Munarin et al., 2015; Fabiola Munarin et al., 2014). The authors observed that gelation time had been strongly affected by HAp particle size, and thus also particle surface area and solubility (F. Munarin et al., 2015). Decreasing particle diameter would increase particle surface area per unit mass. This would in turn lead to an increase in ion release and, presumably, faster gelation. Fast and massive Ca^{2+} ion release from BG structure in aqueous environment (like pectin solution) was confirmed by ICP-OES measurements. This analysis clearly showed that smaller BG particles are capable to release more Ca^{2+} ions compared to bigger ones.

μCT examination revealed BG aggregates in both CA and AA pectin composite hydrogels. The occurrence of aggregation of inorganic particles and their inhomogeneous distribution in hydrogel matrices are commonly known (Leeuwenburgh, Ana, & Jansen, 2010; Leeuwenburgh, Jansen, & Mikos, 2007). It was believed that inhomogeneous distribution of BG particles in AA and CA pectin hydrogel matrices might be ascribed to extremely rapid local crosslinking process of pectin as a consequence of high reactivity of BG particles in

aqueous environment and rapid release of the Ca^{2+} ions. Rapid release of the Ca^{2+} ions would result in the formation of domains of crosslinked pectins around BG agglomerates. Furthermore, less homogeneous distribution of smaller BG particles (2.5 µm) in composite hydrogel matrices can be ascribed to higher release rate of the Ca^{2+} ions, and thus faster pectin gelation (Figure 1B). Pectin crosslinking would stabilize the BG agglomerates and hinder uniform dispersion of BG in the pectin solution, resulting in inhomogeneous distribution. On the one hand, gel-derived bioactive glasses, because of their high surface area, exhibit enhanced chemical reactivity in comparison with conventional melt-derived BG (Mami et al., 2008). On the other hand, the low-methoxyl amidated pectins used in this work require less calcium to form hydrogels than non-amidated LM pectins (Tho, Arne Sande, & Kleinebudde, 2005). The second probable reason for the agglomeration of BG particles could be attributed to their low zeta potential in slightly acidic pH of pectin solutions (Moreira et al., 2014; Fabiola Munarin et al., 2014). When the zeta potential is low, the particles tend to aggregate (Doostmohammadi et al., 2011; Ramos Rivera, Dippel, & Boccaccini, 2018).

The result (Figure 2) reinforces the observation made in previous work that µCT technique are useful tools to study inorganic particle distribution in hydrogel matrices (Douglas et al., 2014, 2016; Douglas, Dziadek, et al., 2018; Douglas, Schietse, et al., 2018; Gorodzha et al., 2016). Hence, one can expect that µCT can be exploited to develop strategies to reduce microparticle aggregation and improve their dispersion.

4.2 In vitro osteoblastic cell response

The results of metabolic activity of the MC3T3-E1 osteoblastic cells cultured for 24 h in direct contact with composite hydrogels as well as microscopic observations indicated the presence of viable cells with a well-spread morphology on the surface of composite

1 hydrogels. This indicated that the composite hydrogels can support cell adhesion. It should be

2 noted that superior cell adhesion was observed on the control (TCPS).

3 The poorer cell adhesion on the composite hydrogels and reduced number of the MC3T3-E1

4 osteoblastic cells (Figure 3A, 3B) might be ascribed to a relatively low stiffness of these

5 materials compared to the control (TCPS). It was previously shown that human mesenchymal

6 stem cells demonstrate an increase in proliferation and cell spreading when cultured on stiff

7 hyaluronic acid hydrogels compared with softer hyaluronic acid hydrogels (Marklein &

8 Burdick, 2010). Similarly, the ability of MC3T3-E1 osteoblastic cells to form focal adhesions

9 was greatly enhanced with increasing stiffness of alginate hydrogels (Baneyx, Baugh, &

10 Vogel, 2002).

11 Another reason might be due to the highly hydrophilic nature of hydrogels, including pectins

12 (Cunha & Gandini, 2010). It is known that highly hydrophilic surfaces prevent the adsorption

13 of cell adhesion-mediating molecules (e.g. vitronectin, fibronectin), or these molecules are

14 bound very weakly (Bacakova, Filova, Parizek, Ruml, & Svorcik, 2011).

15 Furthermore, a reduced number of the cells in direct contact with composite hydrogels and

16 also in undiluted eluates might result from higher local concentrations of Ca^{2+} ions and

17 alkalization near the surfaces of pectin-BG composite hydrogels. It was previously shown that

18 Ca^{2+} ion concentrations above 10 mM have been reported to be cytotoxic (Maeno et al.,

19 2005).

20 A well-spread morphology and high viability of the osteoblastic cells seeded in vicinity of

21 composite hydrogels, as well as large numbers of the cells in 5× and 10× diluted eluates

22 (Figure 3C) would appear to support these hypotheses. The results of *in vitro* cell tests

23 observed in this study are consistent with findings reported in our previous works concerning

24 gellan gum (GG) modified with BG particles of the same chemical composition as used here

(Douglas et al., 2014; Douglas, Dziadek, et al., 2018). The reasons for the greater number of cells cultured in undiluted eluate from CA-2.5 composite hydrogels remain unclear.

Recently, Markov *et al.* demonstrated that low esterified apple pectin inhibits adhesion of J-774 murine macrophages to their surfaces and shows a low cytotoxicity towards NIH3T3 murine fibroblasts (Markov et al., 2017). One of the proposed strategies to improve cell adhesion to the surface of pectin hydrogels and subsequent cell proliferation and differentiation is the chemical grafting of the peptide containing the RGD (Arg-Gly-Asp) integrin-binding sequence onto the pectin molecules (F. Munarin et al., 2011; Fabiola Munarin, Petrini, Tanzi, Barbosa, & Granja, 2012). Therefore, it is possible to obtain multifunctional self-gelling pectin composite hydrogels capable of mineralization with high antibacterial activity and improved cell adhesion.

4.3 Antibacterial testing

It has been demonstrated that bioactive glasses with a high degree of dissolution are likely to show strong antibacterial activity (Zhang et al., 2010). Firstly, this effect may be associated with variations in osmotic pressure, ionic strength, and pH of the environment induced by massive release of the ions (primarily Ca^{2+}) from glass structure. Secondly, the high concentrations of Ca^{2+} could cause perturbations of the membrane potential of bacteria (Munukka et al., 2008; Nazemi et al., 2016). Thus, the strong antibacterial activity of pectin-BG composite hydrogels against MRSA strain Mu50 can be correlated with an increase in Ca^{2+} concentration and alkalization of the bacterial culture medium, confirmed in mineralization studies (Figure 6A). Also in our previous research, strong and extremely fast alkalization of ddH_2O (pH = 11.6) and PBS (pH = 9.5) during zeta potential measurements of BG (at a concentration 1 mg/ml) was reported (Douglas, Dziadek, et al., 2018; Gorodzha et al., 2016). Antibacterial properties of composites observed in this work (Figure 3D) are

significantly enhanced in comparison with GG hydrogels containing bioactive glass particles of the same chemical composition as used in present work (Douglas et al., 2014; Douglas, Dziadek, et al., 2018). In the first case, this can be explained by a much lower amount of BG fillers in GG matrix (1% w/v) (Douglas et al., 2014). However, in the second case the amount of BG particles in GG matrix was the same as used in present work (20% w/v) (Douglas, Dziadek, et al., 2018), therefore the reasons for this effect remain unclear and further studies are needed, also in view of the size of the error bars (Figure 3D).

4.4 Mineralization of composite hydrogels in SBF

Mineralization connected with formation of HAp in composite hydrogels upon incubation in SBF was confirmed directly by SEM/EDX (Figure 4) and FTIR (Figure 5) analyses, and indirectly by the changes in Ca and P content measured using ICP-OES in SBF and samples after incubation (Figures 6A and 6B). ICP-OES analyses indicated massive release of Ca from composite hydrogels glasses of both particle sizes (2.5 µm, <45 µm). However, Ca concentration in SBF and samples was affected both by its release from the glass structure and its uptake resulting from calcium phosphate deposition in materials (Poh, Hutmacher, Stevens, & Woodruff, 2013). Therefore, lower reduction of Ca content in AA and CA composite hydrogels containing BG particles of 2.5 µm size upon immersion in SBF and lower Ca concentration in the solution suggested an enhanced mineralization with respect to the AA-45 and CA-45 composite hydrogels. This can be confirmed by almost total P consumption from SBF and higher P content in both AA-2.5 and CA-2.5 composite hydrogels after incubation. Enhanced mineralization of AA-2.5 and CA-2.5 composite hydrogels could result from the higher surface area of smaller BG particles allowing faster ion exchange with the surrounding medium and consequently enhancing ability of CaP formation (Caridade et al., 2013). Furthermore, BG particles of 2.5 µm size could be more exposed on the surfaces of

composite hydrogels, accelerating dissolution of Ca^{2+} ions from glass structure, leading to faster supersaturation of SBF and therefore faster nucleation and crystallization of calcium phosphate in hydrogels. The results confirmed our previous findings (Douglas, Dziadek, et al., 2018) that the addition of highly bioactive particles, such as bioactive glasses, into hydrogel matrices is a simple way to induce their mineralization in physiological fluids. Furthermore, in this study it was showed that the hydrogel mineralization process depends on the size of bioactive glass particles, i.e. smaller particles promote mineralization better.

5. Conclusions and Outlook

In the present work, novel injectable, self-gelling composites of citrus and apple low esterified amidated pectins modified with gel-derived bioactive glass particles of 2.5 μm and <45 μm sizes were prepared by a simple mixing technique. Bioactive glass particles fulfill three basic functions: they act as delivery vehicle for Ca^{2+} ions for internal pectin crosslinking (i); they display an antibacterial effect (ii) and induce pectin mineralization in a simulated biological environment (iii).

Gelation time depended on BG particle size - smaller particles (<2.5 μm) accelerate gelation slightly faster than bigger ones (<45 μm), which result from higher rate of Ca^{2+} ion release. Microcomputer tomography revealed inhomogeneous distribution of the BG particles in the composite hydrogels. All of the composite hydrogels exhibited strong antibacterial activity against MRSA strain Mu50. Mineralization process of pectin-BG composite hydrogels occurred upon incubation in simulated body fluid for 28 days and depended on glass particle size. Preliminary *in vitro* studies showed that composite hydrogels were cytocompatible with MC3T3-E1 osteoblastic cells.

The pectin-bioactive glass composite hydrogels produced in this work showed great potential for the development of minimally-invasive procedures for bone tissue engineering

applications. However, further studies are needed to improve glass particles distribution in pectin hydrogel matrices, as well as cell attachment to composite hydrogel surfaces.

6. Acknowledgements

7. Conflict of Interest, Ethical Approval, Original Publication, and Author Contribution Statements

The authors have no conflict of interest. No ethical approval was required for this study. No part of this work has been previously published or submitted for publication elsewhere. The authors made the following contributions to the paper:

Timothy E.L. Douglas conceived, designed, planned and coordinated the study, interpreted the data and wrote a large part of the manuscript, under the guidance of Andre G. Skirtach.

Michal Dziadek wrote a large part of the manuscript and together with Katarzyna Cholewa-Kowalska, synthesized bioactive glass particles, conducted incubation in SBF and subsequent SEM (Figure 4), FTIR (Figure 5), as well as ICP-OES analysis (Figure 6A) and interpreted the results.

Josefien Schietse fabricated the pectin-bioactive glass composites, performed rheometric measurements (Figure 1B), and prepared samples for incubation in SBF, as well as μCT, cell biological and microbiological analysis.

Matthieu Boone and Frederic Van Assche performed μCT measurements (Figure 2).

Heidi Declercq performed cell biological characterization (Figures 3A-3C).

Tom Coenye performed antibacterial testing (Figure 3D).

Chris Vervaet and Valérie Vanhoorne performed laser diffraction measurements (Table 1, Figure 1A).

Lieve Balcaen and Frank Vanhaecke performed ICP-OES analysis (Figure 6B).

Maria Buchweitz provided AA and CA pectins.

All authors contributed to writing parts of the paper and provided corrections as appropriate for preparation of the final version of the manuscript.

8. References

Bacakova, L., Filova, E., Parizek, M., Ruml, T., & Svorcik, V. (2011, November). Modulation of cell adhesion, proliferation and differentiation on materials designed for body implants. *Biotechnology Advances*. http://doi.org/10.1016/j.biotechadv.2011.06.004

Baneyx, G., Baugh, L., & Vogel, V. (2002). Fibronectin extension and unfolding within cell matrix fibrils controlled by cytoskeletal tension. *Proceedings of the National Academy of Sciences of the United States of America*, *99*(8), 5139–5143. http://doi.org/10.1073/pnas.072650799

Bosetti, M., Zanardi, L., Hench, L., & Cannas, M. (2003). Type I collagen production by osteoblast-like cells cultured in contact with different bioactive glasses. *Journal of Biomedical Materials Research*, *64A*(1), 189–195. http://doi.org/10.1002/jbm.a.10415

Caridade, S. G., Merino, E. G., Alves, N. M., Bermudez, V. de Z., Boccaccini, A. R., &

Mano, J. F. (2013). Chitosan membranes containing micro or nano-size bioactive glass particles: evolution of biomineralization followed by in situ dynamic mechanical analysis. *Journal of the Mechanical Behavior of Biomedical Materials*, *20*, 173–183. http://doi.org/10.1016/j.jmbbm.2012.11.012

Cui, S., Yao, B., Gao, M., Sun, X., Gou, D., Hu, J., … Liu, Y. (2017). Effects of pectin structure and crosslinking method on the properties of crosslinked pectin nanofibers. *Carbohydrate Polymers*, *157*, 766–774. http://doi.org/10.1016/j.carbpol.2016.10.052

Cunha, A. G., & Gandini, A. (2010, December 1). Turning polysaccharides into hydrophobic materials: A critical review. Part 2. Hemicelluloses, chitin/chitosan, starch, pectin and alginates. *Cellulose*. Springer Netherlands. http://doi.org/10.1007/s10570-010-9435-5

Doostmohammadi, A., Monshi, A., Salehi, R., Fathi, M. H., Golniya, Z., & Daniels, A. U. (2011). Bioactive glass nanoparticles with negative zeta potential. *Ceramics International*, *37*(7), 2311–2316. http://doi.org/10.1016/j.ceramint.2011.03.026

Douglas, T. E. L., Dziadek, M., Gorodzha, S., Lišková, J., Brackman, G., Vanhoorne, V., … Skirtach, A. G. (2018). Novel injectable gellan gum hydrogel composites incorporating Zn- and Sr-enriched bioactive glass microparticles: high-resolution X-Ray micro-computed tomography, antibacterial and in vitro testing. *Journal of Tissue Engineering and Regenerative Medicine*. http://doi.org/10.1002/term.2654

Douglas, T. E. L., Łapa, A., Reczyńska, K., Krok-Borkowicz, M., Pietryga, K., Samal, S. K., … Skirtach, A. G. (2016). Novel injectable, self-gelling hydrogel-microparticle composites for bone regeneration consisting of gellan gum and calcium and magnesium carbonate microparticles. *Biomedical Materials (Bristol)*, *11*(6), 065011. http://doi.org/10.1088/1748-6041/11/6/065011

Douglas, T. E. L., Messersmith, P. B., Chasan, S., Mikos, A. G., de Mulder, E. L. W., Dickson, G., … Leeuwenburgh, S. C. G. (2012). Enzymatic Mineralization of Hydrogels

for Bone Tissue Engineering by Incorporation of Alkaline Phosphatase. *Macromolecular Bioscience*, *12*(8), 1077–1089. http://doi.org/10.1002/mabi.201100501

Douglas, T. E. L., Piwowarczyk, W., Pamula, E., Liskova, J., Schaubroeck, D., Leeuwenburgh, S. C. G., … Dubruel, P. (2014). Injectable self-gelling composites for bone tissue engineering based on gellan gum hydrogel enriched with different bioglasses. *Biomedical Materials (Bristol)*, *9*(4), 045014. http://doi.org/10.1088/1748-6041/9/4/045014

Douglas, T. E. L., Schietse, J., Zima, A., Gorodzha, S., Parakhonskiy, B. V., KhaleNkow, D., … Skirtach, A. G. (2018). Novel self-gelling injectable hydrogel/alpha-tricalcium phosphate composites for bone regeneration: Physiochemical and microcomputer tomographical characterization. *Journal of Biomedical Materials Research - Part A*, *106*(3), 822–828. http://doi.org/10.1002/jbm.a.36277

Dziadek, M., Zagrajczuk, B., Menaszek, E., & Cholewa-Kowalska, K. (2018). A new insight into in vitro behaviour of poly(ε-caprolactone)/bioactive glass composites in biologically related fluids. *Journal of Materials Science*, *53*(6), 3939–3958. http://doi.org/10.1007/s10853-017-1839-2

Francius, G., Hemmerlé, J., Ohayon, J., Schaaf, P., Voegel, J. C., Picart, C., & Senger, B. (2006). Effect of crosslinking on the elasticity of polyelectrolyte multilayer films measured by colloidal probe AFM. *Microscopy Research and Technique*, *69*(2), 84–92. http://doi.org/10.1002/jemt.20275

Gorodzha, S., Douglas, T. E. L., Samal, S. K., Detsch, R., Cholewa-Kowalska, K., Braeckmans, K., … Surmenev, R. A. (2016). High-resolution synchrotron X-ray analysis of bioglass-enriched hydrogels. *Journal of Biomedical Materials Research Part A*, *104*(5), 1194–1201. http://doi.org/10.1002/jbm.a.35642

Hench, L. L. (2009). Genetic design of bioactive glass. *Journal of the European Ceramic*

Society, *29*, 1257–1265. http://doi.org/10.1016/j.jeurceramsoc.2008.08.002

Kim, J. H., Kim, S. H., Kim, H. K., Akaike, T., & Kim, S. C. (2002). Synthesis and characterization of hydroxyapatite crystals: A review study on the analytical methods. *Journal of Biomedical Materials Research*, *62*(4), 600–612. http://doi.org/10.1002/jbm.10280

Kokubo, T., Ito, S., Huang, Z. T., Hayashi, T., Sakka, S., Kitsugi, T., & Yamamuro, T. (1990). Ca, P- rich layer formed on high- strength bioactive glass- ceramic A- W. *Journal of Biomedical Materials Research*, *24*(3), 331–343. http://doi.org/10.1002/jbm.820240306

Laczka, M., Cholewa, K., & Laczka-Osyczka, A. (1997). Gel-derived powders of CaO-P2O5-SiO2 system as a starting material to production of bioactive ceramics. *Journal of Alloys and Compounds*, *248*(1), 42–51. http://doi.org/10.1016/S0925-8388(96)02648-5

Leeuwenburgh, S. C. G., Ana, I. D., & Jansen, J. A. (2010). Sodium citrate as an effective dispersant for the synthesis of inorganic-organic composites with a nanodispersed mineral phase. *Acta Biomaterialia*, *6*(3), 836–844. http://doi.org/10.1016/j.actbio.2009.09.005

Leeuwenburgh, S. C. G., Jansen, J. A., & Mikos, A. G. (2007). Functionalization of oligo(poly(ethylene glycol)fumarate) hydrogels with finely dispersed calcium phosphate nanocrystals for bone-substituting purposes. *Journal of Biomaterials Science, Polymer Edition*, *18*(12), 1547–1564. http://doi.org/10.1163/156856207794761998

Maeno, S., Niki, Y., Matsumoto, H., Morioka, H., Yatabe, T., Funayama, A., … Tanaka, J. (2005, August). The effect of calcium ion concentration on osteoblast viability, proliferation and differentiation in monolayer and 3D culture. *Biomaterials*. http://doi.org/10.1016/j.biomaterials.2005.01.006

Mami, M., Lucas-Girot, A., Oudadesse, H., Dorbez-Sridi, R., Mezahi, F., & Dietrich, E.

(2008). Investigation of the surface reactivity of a sol–gel derived glass in the ternary system SiO2–CaO–P2O5. *Applied Surface Science*, *254*(22), 7386–7393. http://doi.org/10.1016/j.apsusc.2008.05.340

Marklein, R. A., & Burdick, J. A. (2010). Spatially controlled hydrogel mechanics to modulate stem cell interactions. *Soft Matter*, *6*(1), 136–143. http://doi.org/10.1039/B916933D

Markov, P. A., Krachkovsky, N. S., Durnev, E. A., Martinson, E. A., Litvinets, S. G., & Popov, S. V. (2017). Mechanical properties, structure, bioadhesion, and biocompatibility of pectin hydrogels. *Journal of Biomedical Materials Research - Part A*, *105*(9), 2572–2581. http://doi.org/10.1002/jbm.a.36116

Masschaele, B., Dierick, M., Loo, D. Van, Boone, M. N., Brabant, L., Pauwels, E., … Hoorebeke, L. Van. (2013). HECTOR: A 240kV micro-CT setup optimized for research. In *Journal of Physics: Conference Series* (Vol. 463, p. 012012). IOP Publishing. http://doi.org/10.1088/1742-6596/463/1/012012

Moreira, H. R., Munarin, F., Gentilini, R., Visai, L., Granja, P. L., Tanzi, M. C., & Petrini, P. (2014). Injectable pectin hydrogels produced by internal gelation: Ph dependence of gelling and rheological properties. *Carbohydrate Polymers*, *103*(1), 339–347. http://doi.org/10.1016/j.carbpol.2013.12.057

Munarin, F., Guerreiro, S. G., Grellier, M. A., Tanzi, M. C., Barbosa, M. A., Petrini, P., & Granja, P. L. (2011). Pectin-based injectable biomaterials for bone tissue engineering. *Biomacromolecules*, *12*(3), 568–577. http://doi.org/10.1021/bm101110x

Munarin, F., Petrini, P., Barcellona, G., Roversi, T., Piazza, L., Visai, L., & Tanzi, M. C. (2014). Reactive hydroxyapatite fillers for pectin biocomposites. *Materials Science and Engineering C*, *45*, 154–161. http://doi.org/10.1016/j.msec.2014.09.003

Munarin, F., Petrini, P., Gentilini, R., Pillai, R. S., Dirè, S., Tanzi, M. C., & Sglavo, V. M.

(2015). Micro- and nano-hydroxyapatite as active reinforcement for soft biocomposites. *International Journal of Biological Macromolecules*, *72*, 199–209. http://doi.org/10.1016/j.ijbiomac.2014.07.050

Munarin, F., Petrini, P., Tanzi, M. C., Barbosa, M. A., & Granja, P. L. (2012). Biofunctional chemically modified pectin for cell delivery. *Soft Matter*, *8*(17), 4731. http://doi.org/10.1039/c2sm07260b

Munukka, E., Leppäranta, O., Korkeamäki, M., Vaahtio, M., Peltola, T., Zhang, D., … Eerola, E. (2008). Bactericidal effects of bioactive glasses on clinically important aerobic bacteria. *Journal of Materials Science: Materials in Medicine*, *19*(1), 27–32. http://doi.org/10.1007/s10856-007-3143-1

Nazemi, Z., Mehdikhani-Nahrkhalaji, M., Haghbin-Nazarpak, M., Staji, H., & Kalani, M. M. (2016). Antibacterial activity evaluation of bioactive glass and biphasic calcium phosphate nanopowders mixtures. *Applied Physics A: Materials Science and Processing*, *122*(12), 1063. http://doi.org/10.1007/s00339-016-0587-5

Neves, S. C., Gomes, D. B., Sousa, A., Bidarra, S. J., Petrini, P., Moroni, L., … Granja, P. L. (2015). Biofunctionalized pectin hydrogels as 3D cellular microenvironments. *Journal of Materials Chemistry B*, *3*(10), 2096–2108. http://doi.org/10.1039/C4TB00885E

Poh, P. S. P., Hutmacher, D. W., Stevens, M. M., & Woodruff, M. A. (2013). Fabrication and *in vitro* characterization of bioactive glass composite scaffolds for bone regeneration. *Biofabrication*, *5*(4), 045005. http://doi.org/10.1088/1758-5082/5/4/045005

Popov, S. V, Popova, G. Y., Nikitina, I. R., Markov, P. A., Latkin, D. S., Golovchenko, V. V, … Litvinets, S. G. (2016). Injectable hydrogel from plum pectin as a barrier for prevention of postoperative adhesion. *Journal of Bioactive and Compatible Polymers*, *31*(5), 481–497. http://doi.org/10.1177/0883911516637374

Ramos Rivera, L., Dippel, J., & Boccaccini, A. R. (2018). Formation of Zein/Bioactive Glass

Layers Using Electrophoretic Deposition Technique. *ECS Transactions*, *82*(1), 73–80. http://doi.org/10.1149/08201.0073ecst

Secchi, E., Munarin, F., Alaimo, M. D., Bosisio, S., Buzzaccaro, S., Ciccarella, G., … Piazza, R. (2014). External and internal gelation of pectin solutions: Microscopic dynamics versus macroscopic rheology. *Journal of Physics Condensed Matter*, *26*(46), 464106. http://doi.org/10.1088/0953-8984/26/46/464106

Silver, I. A., Deas, J., & Erecińska, M. (2001). Interactions of bioactive glasses with osteoblasts in vitro: effects of 45S5 Bioglass®, and 58S and 77S bioactive glasses on metabolism, intracellular ion concentrations and cell viability. *Biomaterials*, *22*(2), 175–185. http://doi.org/10.1016/S0142-9612(00)00173-3

Stratton, S., Shelke, N. B., Hoshino, K., Rudraiah, S., & Kumbar, S. G. (2016). Bioactive polymeric scaffolds for tissue engineering. *Bioactive Materials*, *1*(2), 93–108. http://doi.org/10.1016/j.bioactmat.2016.11.001

Tho, I., Arne Sande, S., & Kleinebudde, P. (2005). Cross-linking of amidated low-methoxylated pectin with calcium during extrusion/spheronisation: Effect on particle size and shape. *Chemical Engineering Science*, *60*(14), 3899–3907. http://doi.org/10.1016/j.ces.2005.02.023

Volodkin, D. V., Delcea, M., Möhwald, H., & Skirtach, A. G. (2009). Remote near-IR light activation of a hyaluronic acid/poly(l -lysine) multilayered film and film-entrapped microcapsules. *ACS Applied Materials and Interfaces*, *1*(8), 1705–1710. http://doi.org/10.1021/am900269c

Yuliarti, O., Hoon, A. L. S., & Chong, S. Y. (2017a). Influence of pH, pectin and Ca concentration on gelation properties of low-methoxyl pectin extracted from Cyclea barbata Miers. *Food Structure*, *11*, 16–23. http://doi.org/10.1016/J.FOOSTR.2016.10.005

1   Yuliarti, O., Hoon, A. L. S., & Chong, S. Y. (2017b). Microstructure and kinetic rheological

2   behavior of amidated and nonamidated LM pectin gels. *Food Structure*, *11*(1), 16–23.

3   http://doi.org/10.1021/bm050459r

4   Zhang, D., Leppäranta, O., Munukka, E., Ylänen, H., Viljanen, M. K., Eerola, E., … Hupa, L.

5   (2010). Antibacterial effects and dissolution behavior of six bioactive glasses. *Journal of*

6   *Biomedical   Materials   Research   -   Part   A*,   *93*(2),   475–483.
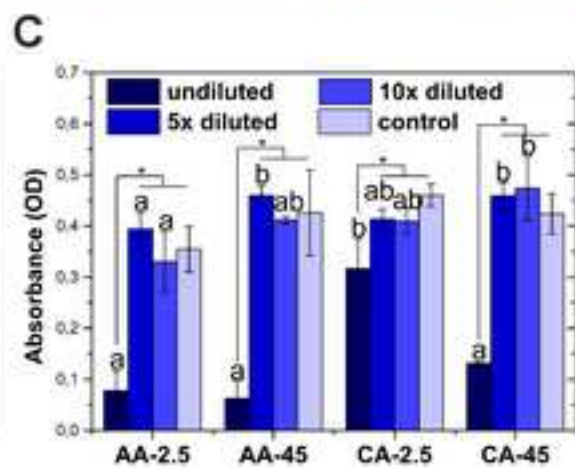
7   http://doi.org/10.1002/jbm.a.32564

8
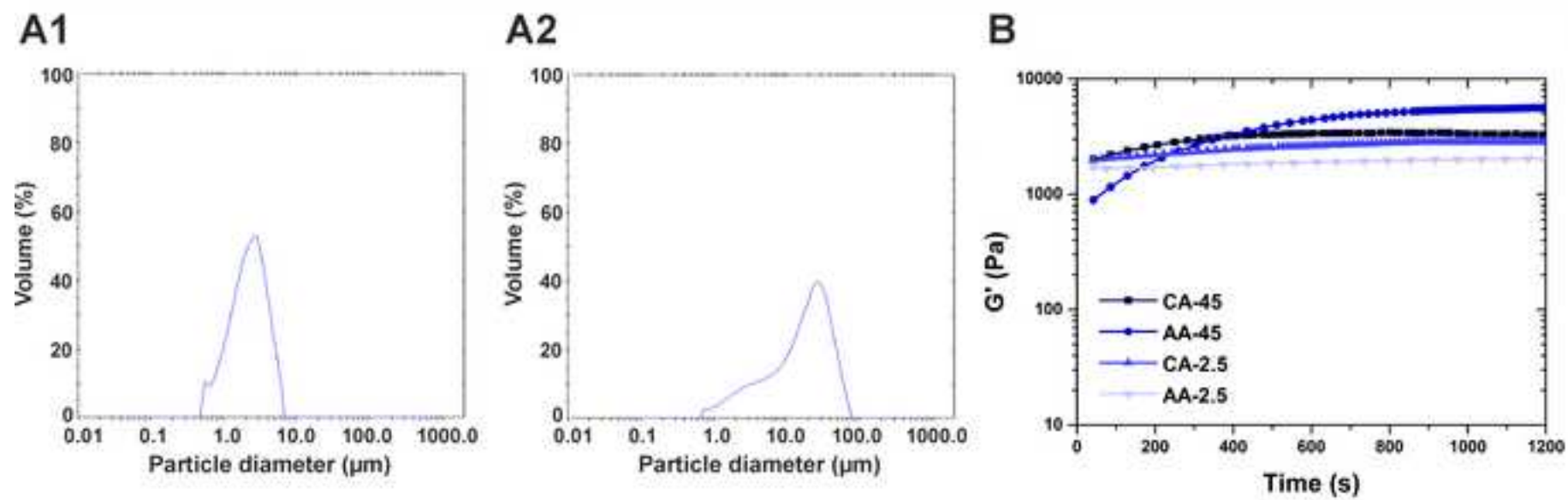
Figure 2
[Click here to download high resolution image](#)
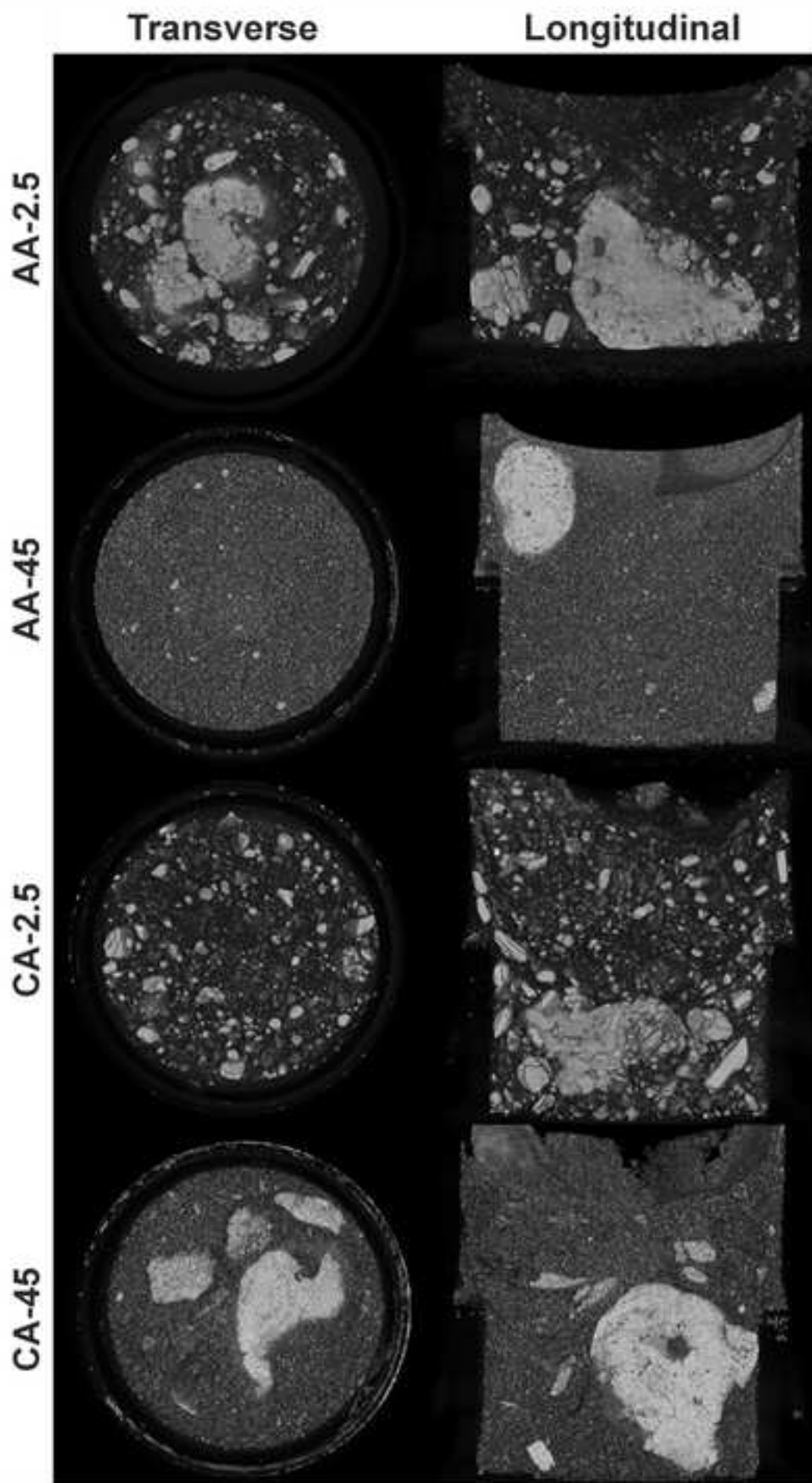
Figure 3
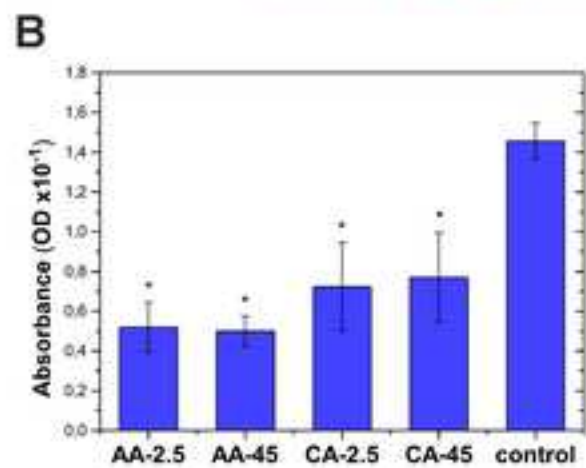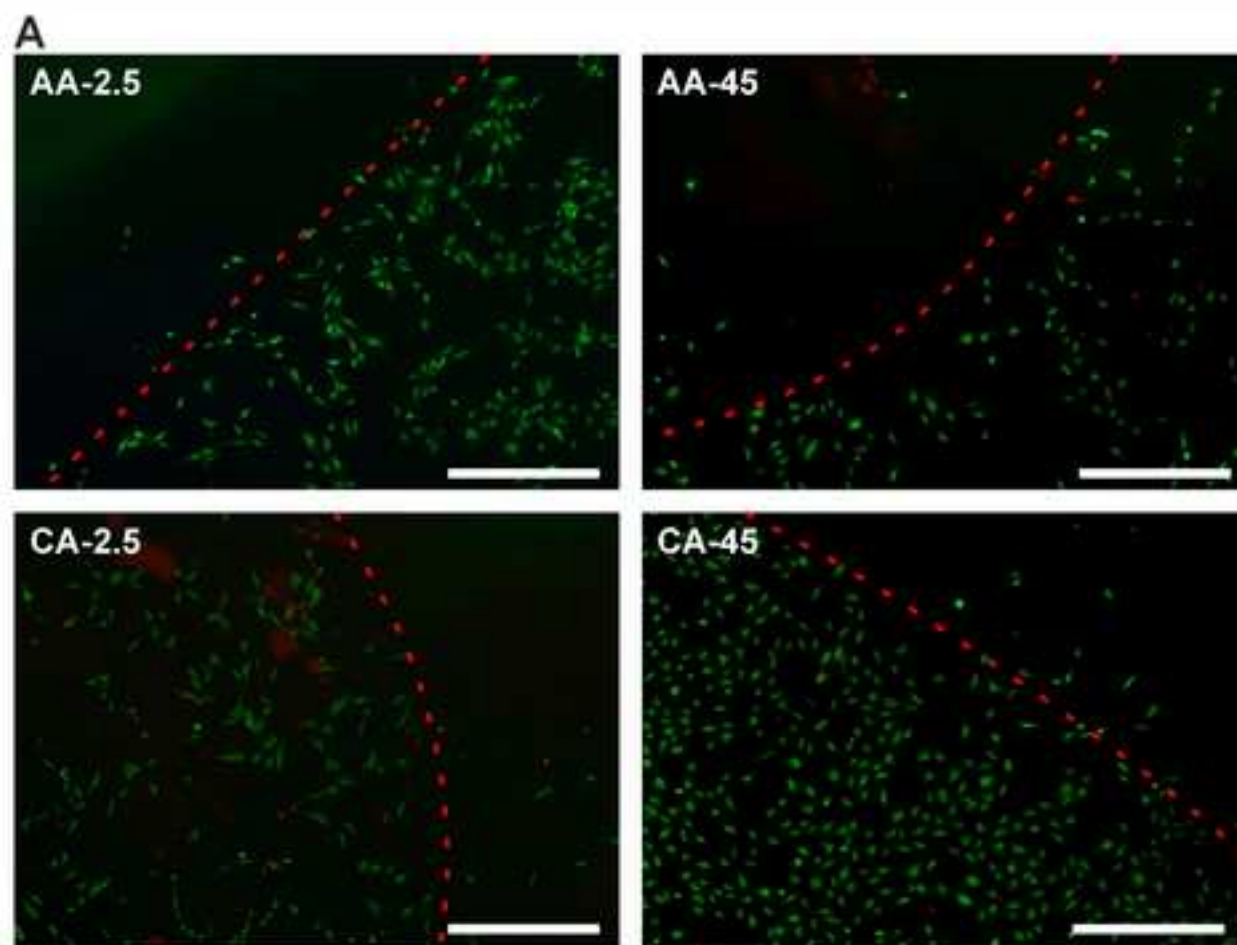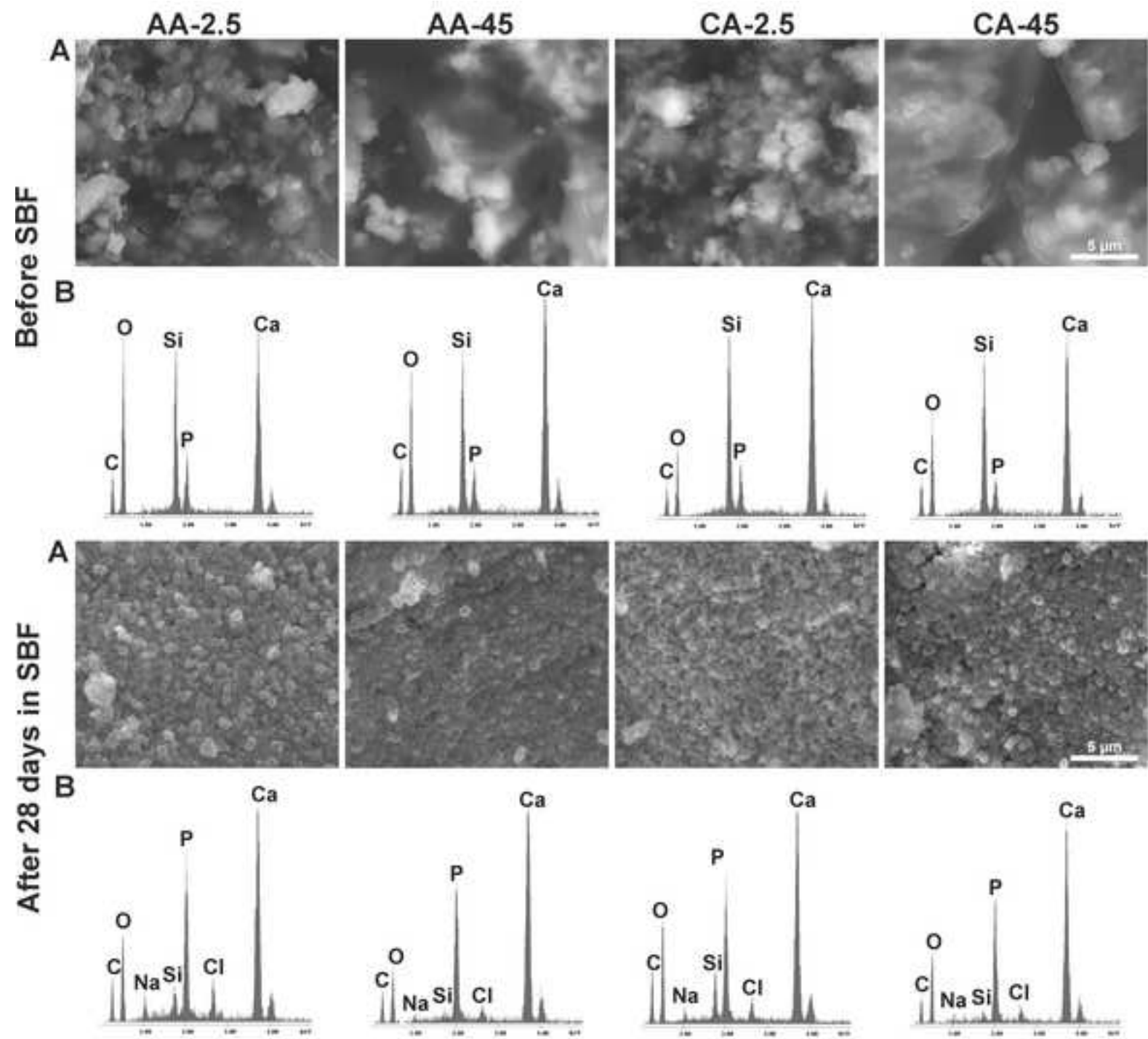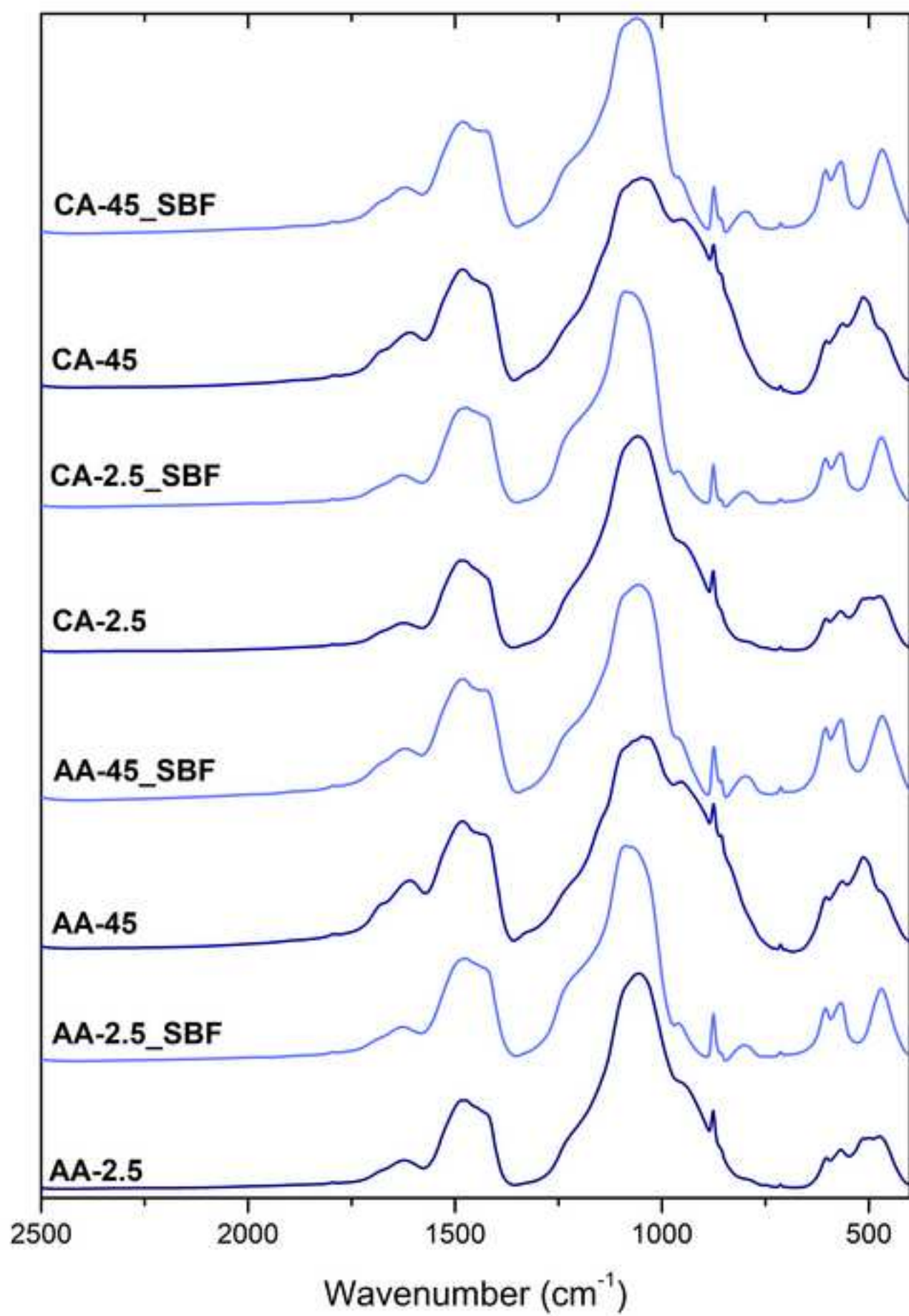**Click here to download high resolution image**

Figure 4

Figure 5

Pectin solution
(from citrus peels
and apple pomace)

+

Bioactive glass particles
(2.5 μm and <45 μm)

Ca²⁺ ion release

Internal pectin
crosslinking

Ca^{2+} ions

Crosslinked
composite hydrogel

Distribution of bioactive
glass particles - μCT

Mineralization in SBF

MC3T3-E1 osteoblastic
cell response

Antibacterial activity
against MRSA